THE PUBLISHING HOUSE
OF THE ROMANIAN ACADEMY

PROCEEDINGS OF THE ROMANIAN ACADEMY, Series A,
Volume 25, Number 1/2024, pp. 75–86
DOI: 10.59277/PRA-SER.A.25.1.10

DISTURBANCE OBSERVER-BASED FIXED TIME CONTROL FOR BIDIRECTIONAL DC-DC CONVERTER WITH INPUT VOLTAGE AND LOAD UNCERTAINTY

Xiaolong TIAN[1], Fazhan TAO[1,3], Zhumu FU[1,2], Shuzhong SONG[1], Nan WANG[1]

[1] Henan University of Science and Technology, College of Information Engineering, NO.263 Kaiyuan Road, Luoyang, 471023, Henan, China
[2] Henan University of Science and Technology, Henan Key Laboratory of Robot and Intelligent Systems, NO.263 Kaiyuan Road, Luoyang, 471023, Henan, China
[3] Longmen Laboratory, Luoyang, 471023, Henan, People's Republic of China
Corresponding author: Zhumu Fu, E-mail: fuzhumu@haust.edu.cn

Abstract. The bidirectional DC-DC converter serves a vital role in the energy recovery system of new energy vehicles. However, external interference and parameter uncertainty can easily affect its dynamic performance. A disturbance observer-based fixed time control strategy for bidirectional DC-DC is proposed to address the impact of input voltage and load uncertainty on bidirectional converters. Firstly, the bidirectional converter model undergoes coordinate transformation, and disturbance observers are designed to compensate for input voltage and load disturbances. Secondly, based on the fixed time control theory, a fixed-time controller is devised for the bidirectional DC-DC converter to facilitate fast tracking and adjustment of output voltage without requiring measurement of input voltage and load current. Finally, simulation and experiment evaluations are conducted to assess the proposed scheme's effectiveness in output voltage regulation.

Keywords: bidirectional DC-DC, fixed time control, disturbance observer, load uncertainty.

1. INTRODUCTION

The bidirectional converter is a widely used switching power converter in various fields such as new energy vehicle power systems, photovoltaic energy storage, wind power storage systems, and aerospace applications. It offers advantages such as high power density, bidirectional power flow, and easy integration [1]. The main control objective in these applications is to ensure that the output voltage can quickly track the reference voltage. However, achieving this objective is often hindered by multiple factors. On one hand, changes in load resistance are inevitable, while on the other hand, interference caused by variations in input voltage is common. The presence of these two factors can significantly degrade the control performance of the system. Therefore, it is crucial to design a controller with robust anti-interference capability and fast dynamic response to address these challenges.

To address the challenges associated with output voltage control in bidirectional DC-DC converters, extensive research has been conducted by scholars and researchers, resulting in the proposal of various effective control methods. These include traditional PID control [2–3], fuzzy logic-based control [4–7], and sliding mode control [8–9]. The PID control method is commonly used due to its simplicity in controller design and implementation without the requirement of a system model. However, it heavily relies on manual experience for parameter tuning, which can lead to decreased accuracy or even failure if there is a mismatch between the controller parameters and the system's characteristics. To overcome these drawbacks, researchers have proposed a fuzzy logic-based control method [4–7] that exhibits strong adaptability to DC-DC converter systems with inherent delay and nonlinear characteristics, although accurate system models are necessary. However, this method struggles to handle high load uncertainty interference. Sliding mode control has been adopted by scholars in DC-DC converters due to its insensitivity to parameter uncertainty and external disturbances [8–9], enhancing the robustness of bidirectional converter systems. Nevertheless, traditional sliding mode control has two main drawbacks: firstly, the output voltage can only exponentially converge to zero within infinite time; secondly, the controller's discontinuity results in chattering around the sliding mode surface, making it vulnerable to failure in the presence of load disturbances. To tackle these issues, researchers have gradually employed higher-order sliding mode methods [10], non-singular terminal sliding mode control methods [11], and integral sliding mode control methods [12–13]. These methods help reduce chattering effects while maintaining the excellent performance of traditional sliding mode control. However, they still face limitations in guaranteeing control effectiveness during significant load disturbances. In order to improve the convergence performance and disturbance resistance of the continuous system, scholars have studied and developed finite time control methods based on continuous state feedback [14–15]. By using this method, the state of the system can converge to the equilibrium point within a finite time when there is no external interference in the system. When there is external interference in the system, utilizing its non-smooth characteristics can improve the anti-interference performance of the closed-loop system. Compared with sliding mode control, finite time control belongs to continuous state feedback, which avoids phenomena such as chattering in practical applications. In [16], a combination of fixed time and finite time observers is applied in the Buck circuit to improve its transient response capability.

With the advancements in observer research and their application, various types of observers have been proposed to estimate converter interference. Examples include extended observers [17–19], disturbance observers [20–21], and high-order sliding mode observers [23]. These observers effectively compensate for performance degradation caused by external interference and model parameter uncertainty. The extended observer treats disturbance as an additional state of the system, estimating both the state and disturbance through simple calculations. The disturbance estimation is then utilized by the controller to compensate for system performance, specifically addressing the issue of mismatched disturbances in sliding mode control and achieving improved disturbance suppression capabilities [17–19]. To further enhance the converter's anti-interference ability, the combination of sliding mode control and disturbance observer has been explored. This approach tackles uncertainties arising from both matched and mismatched disturbances, resulting in stronger robustness to external interferences compared to extended observers. However, studies conducted in [20–22] reveal that disturbances in the bidirectional converter model exist across different state equations and are considered as mismatched disturbances. Consequently, effectively suppressing the impact of such disturbances comes at the cost of sacrificing controller performance. Additionally, the inclusion of additional voltage or current sensors leads to higher system costs. As a result, researchers have explored the use of disturbance observers and high-order sliding mode observation techniques to reduce the number of sensors while simultaneously achieving disturbance compensation [23].

However, it is worth noting that the above research on DC-DC converters mostly focuses on unidirectional DC-DC converters. The use of sliding mode methods inevitably leads to chattering [12, 17, 18], which will additionally increase the burden of high-frequency switching on high-power converters. Although the application of disturbance observer has good results, it cannot effectively improve the fast tracking performance of the system due to the lack of effective integration with fixed time control. Since the disturbance observer can effectively compensate for the degradation of DC-DC converter system performance caused by external disturbances and parameter uncertainties, while the fixed time controller which is independent of the initial state cannot only further improve the system's anti-interference ability, but also accelerate the tracking speed of the system's output voltage. Therefore, the combination of the two can achieve stronger robustness and convergence performance of the system. In view of this, this paper proposes a fixed time control strategy based on disturbance observer to solve the problem of control performance degradation caused by input voltage and load changes in bidirectional DC-DC converters. Compared to previous research, the main innovation of this article lies in the voltage regulation of bidirectional DC-DC, which not only compensates for external disturbances but also improves the speed of tracking load voltage.

The main contributions of this paper are summarized as follows:

1) A disturbance observer is proposed to compensate for the impact of both input voltage and load disturbances on the bidirectional DC-DC converter system. By transforming the system into standard forms of mismatched and matched disturbance system, the disturbance terms are designed to account for input voltage and load uncertainties separately. A specific form of disturbance observer is devised, and the asymptotic convergence of the observer is proven.

2) A combination of the previously mentioned disturbance observer and fixed-time control is introduced to enhance the system's dynamic response. Leveraging the estimated values from the designed observer, a

control law is constructed using a fixed time controller. To improve the system's dynamic response, the backstepping method, along with fixed time theory, is employed for controller design, ensuring stability of the system.

3) Simulation and experiment results verify the fast response capability of the proposed controller to input voltage and load disturbances. Compared to PID controller, the proposed approach improves the output voltage tracking speed by 5% and reduces the ripple of the output current by 10%.

The remaining parts of this paper are as follows. Section 2 describes the problem statements including the model of bidirectional DC-DC converter and the preliminary knowledge. Section 3 presents the design of fixed time controller based on disturbance observer. Section 4 shows the simulation and experiment results. The main conclusions of this paper are drawn in Section 5.

2. PROBLEM STATEMENTS

2.1. The model of bidirectional DC-DC converter

The bidirectional converter [23], as illustrated in Fig. 1, consists of a load resistor (R), an inductor (L), and a capacitor (C). The diode (D_1, D_2) and MOSFET transistors (Sw_1, Sw_2) are also present in the circuit. v_g is the input voltage; i_L is the inductance current, and the voltage on the capacitor is equal to the output voltage v_o. It should be noted that the input voltage (v_g) and load resistance (R) are unknown but lie within a certain range. The control objective is to regulate v_o to achieve the desired voltage (v_{ref}) in the presence of load uncertainty. The control objective is to achieve rapid and stable adjustment of the output voltage (v_o) to the reference voltage (v_{ref}) under input voltage and load disturbances.

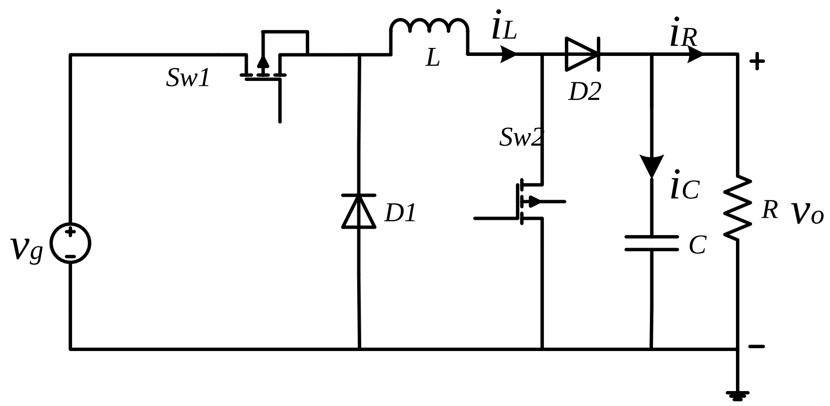

Fig. 1 – Bi-directional DC-DC Converter.

Assuming u is the duty cycle of the control input, then the state space average model of the bidirectional converter in continuous conduction mode [23] is

$$\begin{aligned}\frac{\mathrm{d}i_L}{\mathrm{d}t} &= \frac{v_g}{L}u - (1-u)\frac{v_o}{L}\\ \frac{\mathrm{d}v_o}{\mathrm{d}t} &= -\frac{v_o}{RC} + (1-u)\frac{i_L}{C}\end{aligned} \tag{1}$$

In the modeling of bidirectional DC-DC converters, it is common to choose the inductor current and capacitor voltage as state variables, denoted as $x_1 = i_L$ and $x_2 = V_o$. The system model of the bidirectional DC-DC converter can be reformulated as follows:

$$\begin{aligned}\dot{x}_1 &= \frac{v_g}{L}u - (1-u)\frac{x_2}{L}\\ \dot{x}_2 &= -\frac{x_2}{RC} + (1-u)\frac{x_1}{C}\end{aligned} \tag{2}$$

By performing coordinate transformation on the equation above, we obtain

$$\begin{gathered}\dot{z}_1 = a'_{11}(z_2 + v_{ref} + k_1)u + \omega_1 \\ \dot{z}_2 = a'_{21}z_1 + \omega_2 \\ \omega_1 = -a'_{11}(z_2 + v_{ref} + k_1 u - v_g u) \\ \omega_2 = -a'_{21}\left(uz_1 + \frac{z_2 + v_{ref}}{R}\right)\end{gathered} \tag{3}$$

where $a'_{11} = \frac{1}{L}$, $a'_{21} = \frac{1}{C}$, $z_1 = i_L$, $z_2 = v_0 - v_{ref}$; a'_{11} and a'_{21} are known constants; ω_1 and ω_2 have uncertain perturbation terms, and k_1 is the normal number selected by the user. Equation (3) serves as the standard form for mismatched and matched disturbance systems, with input voltage and load uncertainties pushed to disturbances ω_1 and ω_2.

Bidirectional converters are mainly used for voltage regulation. In addition to considering the steady-state accuracy of the output voltage, it is also necessary to consider the dynamic performance of the output voltage. Especially when there are load changes and input voltage fluctuations, it is particularly important to maintain accurate and fast voltage tracking. Due to the uncertainty of input voltage v_g and load resistance R, ω_1 and ω_2 are also uncertain terms. The objective is to design a new control law that enables the output voltage to track the reference value quickly and stably in the presence of uncertainties in the system.

2.2. Preliminary knowledge

LEMMA 1 [15]. *Suppose a nonlinear system (2) is considered, assuming the presence of a continuous positive definite Lyapunov function $V(x)$. If its derivative satisfies the following conditions:*

$$\dot{V}(x) \leq -\alpha V(x)^{\gamma_1} - \beta V(x)^{\gamma_2} \tag{4}$$

where constants $\alpha, \beta > 0$, $0 < \gamma_1 < 1$, $\gamma_2 > 1$, then the origin of the system is globally fixed time stable, and the convergence time T satisfies:

$$T \leq T_{max} := \frac{1}{\alpha(1-\gamma_1)}\frac{1}{\beta(\gamma_2 - 1)}. \tag{5}$$

Note. T_{max} is the upper bound of convergence time. To facilitate the controller design process, we set $\gamma_1 = \frac{1}{2}$ and $\gamma_2 = 2$, while α, β can be adjusted accordingly based on specific requirements.

LEMMA 2 (Cauchy Schwartz inequality) [24]. *For any $m > 0, i = 1, \ldots, n$, the following inequality holds:*

$$\left(\sum_{i=1}^{n} m_i\right)^2 \leq n \sum_{i=1}^{n} {m_i}^2. \tag{6}$$

3. DESIGN OF FIXED TIME CONTROLLER BASED ON DISTURBANCE OBSERVER

To fulfill the control requirements of DC-DC converters and address variations in input voltage and load resistance, a novel control algorithm is developed by integrating disturbance observer with fixed-time control. The disturbance observer is utilized to estimate the converter's input voltage and load resistance values, which are then fed back to a fixed-time controller to establish a control law. The design diagram of a disturbance observer based fixed time controller for bidirectional DC-DC converters is shown in Fig. 2.

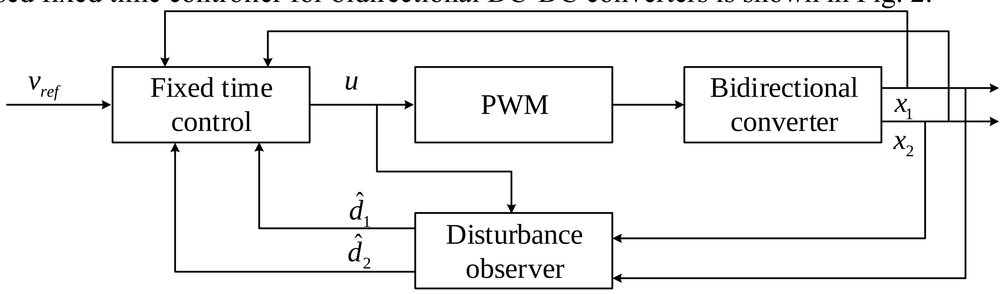

Fig. 2 – Fixed time controller based on disturbance observer for Bidirectional DC-DC Converter.

3.1. Design of disturbance observer

The primary purpose of the disturbance observer is to provide real-time estimation for two uncertain terms, denoted as ω_1 and ω_2. Let $\widehat{\omega}_1$and $\widehat{\omega}_2$ represent the estimated values of ω_1 and ω_2, respectively. $\widetilde{\omega}_1 = \omega_1 - \widehat{\omega}_1$, $\widetilde{\omega}_2 = \omega_2 - \widehat{\omega}_2$ are defined as the estimation errors.

1) The observer design for disturbance $\boldsymbol{\omega_1}$ is as follows:

$$\begin{aligned} \widehat{\omega}_1 &= p_1 + l_1 z_1 \\ \dot{p}_1 &= -l_1(a'_{11}(z_2 + v_{ref} + k_1)u + \widehat{\omega}_1) \end{aligned} \tag{7}$$

$$\dot{\widehat{\omega}}_1 = l_1 \widetilde{\omega}_1 \tag{8}$$

where l_1 is the observer gain and p_1 is the auxiliary state variable.

By substituting (8) into $\dot{\widetilde{\omega}}_1$, we have

$$\dot{\widetilde{\omega}}_1 = \dot{\omega}_1 - \dot{\widehat{\omega}}_1 = \dot{\omega}_1 - l_1 \widetilde{\omega}_1. \tag{9}$$

2) The observer design for disturbance ω_2 is as follows:

$$\begin{aligned} \widehat{\omega}_2 &= p_2 + l_2 z_2 \\ \dot{p}_2 &= -l_2(a'_{21} z_1 + \widehat{\omega}_2) \end{aligned} \tag{10}$$

$$\dot{\widehat{\omega}}_2 = l_2 \widetilde{\omega}_2 \tag{11}$$

where l_2 is the observer gain and p_2 is the auxiliary state variable.

By substituting (11) into $\dot{\widetilde{\omega}}_2$, we have

$$\dot{\widetilde{\omega}}_2 = \dot{\omega}_2 - \dot{\widehat{\omega}}_2 = \dot{\omega}_2 - l_2 \widetilde{\omega}_2 \,. \tag{12}$$

From (9) and (12), when ω_1, ω_2 are constant, the estimation error will gradually converge to zero, and its convergence rate is determined by the observer gains l_1, l_2. In a bidirectional DC-DC converter system, the changes in input voltage and load resistance vary in a stepped manner at certain time points. In other cases, their values can be considered constant. Based on $l_1, l_2 > 0$, the estimation error is asymptotically stable.

3.2. Fixed time controller design

Based on the above estimation of disturbances, this section employs the backstepping method to derive the switching control conditions for the bidirectional DC-DC converter through the following two steps.

THEOREM 1. *For the system (3), if the controller satisfies the following conditions*

$$u = \frac{a'_{21}\omega_1 + \dot{\omega}_2 + 3m_2 z_2^2 \dot{z}_2 + m_3 \operatorname{sgn}(e_1) + m_4 e_1^3}{-a'_{21}a'_{11}(z_2 + v_{ref} + k_1)}, \tag{13}$$

then the state of the system converges to 0 *in a fixed time.*

Proof. Step 1 is based on the dynamic model of the bidirectional DC-DC converter. The first design goal is to track the reference voltage v_{ref} with the output voltage v_o, which minimizes the error $z_2 = v_o - v_{ref}$. The convergence of the error can be analyzed by constructing the following Lyapunov function:

$$V_1 = \frac{1}{2} z_2^2. \tag{14}$$

By taking the derivative of (14), we have:

$$\dot{V}_1 = z_2 \dot{z}_2 = z_2(a'_{21} z_1 + \omega_2). \tag{15}$$

To achieve the condition $v_o = v_{ref}$, it is necessary to select the appropriate function z_1 so that $\dot{W}_1$ satisfies the fixed time *Lemma 1*, and then the error z_2 converges to zero within a fixed time. For this purpose, the design z_1 is as follows:

$$a'_{21} z_1 + \omega_2 = -m_1 \operatorname{sgn}(z_2) - m_2 z_2^3. \tag{16}$$

Note. m_σ is positive number ($\sigma = 1,\dots,6$).

Hence, (15) can be simplified as

$$\dot{V}_1 = -m_1 z_2 \operatorname{sgn}(z_2) - m_2 z_2^4. \tag{17}$$

Step 2. In order to find a suitable z_1 that meets the above conditions, the associated error variables are defined as follows:

$$e_1 = a'_{21} z_1 + \omega_2 + m_1 \operatorname{sgn}(z_2) + m_2 z_2^3. \tag{18}$$

By taking the derivative of (18), we have

$$\dot{e}_1 = a'_{21}\dot{z}_1 + \dot{\omega}_2 + 3m_2 z_2^2 \dot{z}_2. \tag{19}$$

By substituting (3) into (19), we have

$$\begin{aligned} \dot{e}_1 &= a'_{21}\dot{z}_1 + \dot{\omega}_2 + 3m_2 z_2^2 \dot{z}_2 = \\ &= a'_{21}a'_{11}(z_2 + v_{ref} + k_1)u + a'_{21}\omega_1 + \dot{\omega}_2 + 3m_2 z_2^2 \dot{z}_{2_1} \end{aligned} \tag{20}$$

The convergence of e_1 can be analyzed by constructing the following Lyapunov function

$$V_3 = \frac{1}{2} z_2^2 + \frac{1}{2} e_1^2. \tag{21}$$

where $V_2 = \frac{1}{2} e_1^2$.

By taking the derivative of (21), we have

$$\dot{V}_3 = -m_1 z_2 \operatorname{sgn}(z_2) - m_2 z_2^4 + e_1 \dot{e}_1. \tag{22}$$

Consequently, when (20) satisfies the following conditions

$$a'_{21}a'_{11}(z_2 + v_{ref} + k_1)u + a'_{21}\omega_1 + \dot{\omega}_2 + 3m_2 z_2^2 \dot{z}_2 = -m_3 \operatorname{sgn}(e_1) - m_4 e_1^3, \tag{23}$$

Equation (22) can be simplified as:

$$\begin{aligned} \dot{V}_3 &= z_2\dot{z}_2 + e_1\dot{e}_1 = -m_1 z_2 \operatorname{sgn}(z_2) - m_2 z_2^4 - m_3 e_1 \operatorname{sgn}(e_1) - m_4 e_1^4 = \\ &= -m_1 V_1^{\frac{1}{2}} - m_2 V_1^2 - m_3 V_2^{\frac{1}{2}} - m_4 V_2^2 \end{aligned} \tag{24}$$

At this point, the controller input u meets the following conditions

$$u = \frac{a'_{21}\omega_1 + \dot{\omega}_2 + 3m_2 z_2^2 \dot{z}_2 + m_3 \operatorname{sgn}(e_1) + m_4 e_1^3}{-a'_{21}a'_{11}(z_2 + v_{ref} + k_1)}. \tag{25}$$

From *Lemma 2*, it can be concluded that

$$\begin{aligned} \dot{V}_3 &= -m_1 V_1^{\frac{1}{2}} - m_2 V_1^2 - m_3 V_2^{\frac{1}{2}} - m_4 V_2^2 \\ &\le -m_5 (V_1^{\frac{1}{2}} + V_2^{\frac{1}{2}}) - m_6 (V_1^2 + V_2^2) \\ &\le -m_5 (V_1 + V_2)^{\frac{1}{2}} - m_6 (V_1 + V_2)^2 \end{aligned} \tag{26}$$

Note: $m_5 = \min(m_1, m_3)$, $m_6 = \min(m_2, m_4)$.

Proof completed. Under the influence of the controller, the system state adheres to the *Theorem 1*, ensuring convergence of all states to the desired value within a fixed time. As a result, the output voltage can efficiently track the reference voltage value.

Remark 1. The control performance of the system is dependent on many devise parameters. Based on stability analysis, it can be known that the parameters $m_5 = \min(m_1, m_3)$, $m_6 = \min(m_2, m_4)$ can adjust the tracking error and tracking accuracy simultaneously. By choosing larger m_5 and m_6, the tracking velocity can be advanced and the steady-state error can be reduced. Besides, the exponents γ_1 and γ_2 determine the boundary of the settling time and affect the tracking accuracy. Selecting appropriate exponents can shorten the convergence time and enhance the tracking accuracy.

4. SIMULATION AND EXPERIMENT RESULTS

To evaluate the effectiveness of the proposed composite controller, simulations are performed using MATLAB/Simulink, and experimental validation is carried out on the dSPACE1202 experimental platform. Table 1 displays the system parameters utilized in the Simulink simulations, while Table 2 presents the corresponding controller parameters. The control objective is to verify the tracking effect of output voltage under changes in load or input voltage. A commonly employed PID control strategy is used for comparative purposes.

Table 1

System parameter

Descriptions	Values	Units
Input voltage	40	V
Reference voltage	25	V
Load resistance	10	Ω
Inductor	330	μH
Capacitor	140	μF

Table 2

Controller parameters

Controllers	Parameters
Fixed time controller	$m_2 = 100,\ m_3 = 10\ 000,\ m_4 = 2\ 500$
PID controller	$P = 0.1, I = 150$

4.1. Simulation results

1) *Simulation under load changes*. To assess the tracking ability of the proposed controller and PID controller in relation to output voltage and output current ripple under varying load resistance, a load transition from 10 Ω to 13 Ω is implemented at 1 ms. Fig. 3 reveals the performance of the proposed fixed time controller in terms of output voltage tracking. The fluctuation amplitude around the reference voltage of 25 V remained within 1 V at 1 ms and rapidly converged back to 25 V within 1.1 ms. Compared to the PID control, the proposed controller exhibits superior characteristics with a faster response speed (increased by 26.6%) and reduced overshoot (decreased by 5.86%). Furthermore, Fig. 4 indicates that the fixed time controller generates significantly smaller output current ripple compared to the PID control when subjected to load resistance variations. This reduced current ripple holds great importance for both the load and the power supply, contributing to an enhanced service life of the power supply.

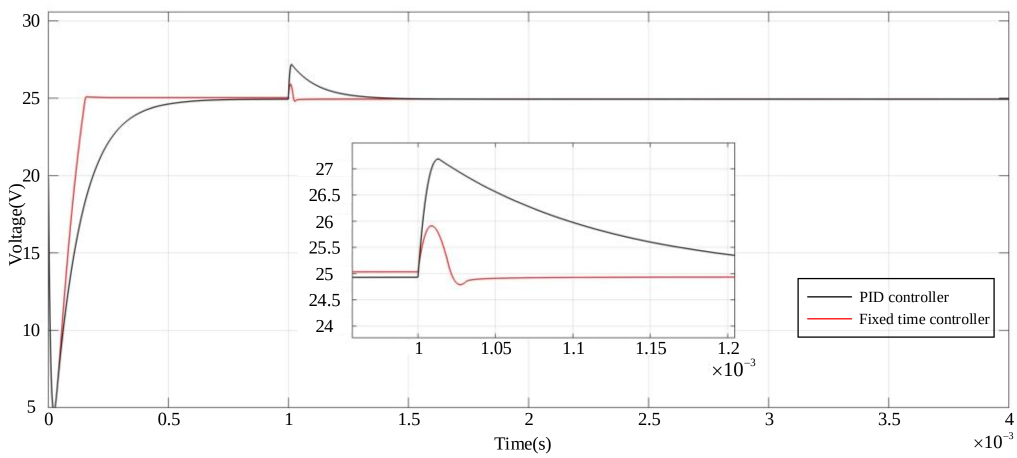

Fig. 3 – Comparison of output voltage tracking effects between two controllers under load changes.

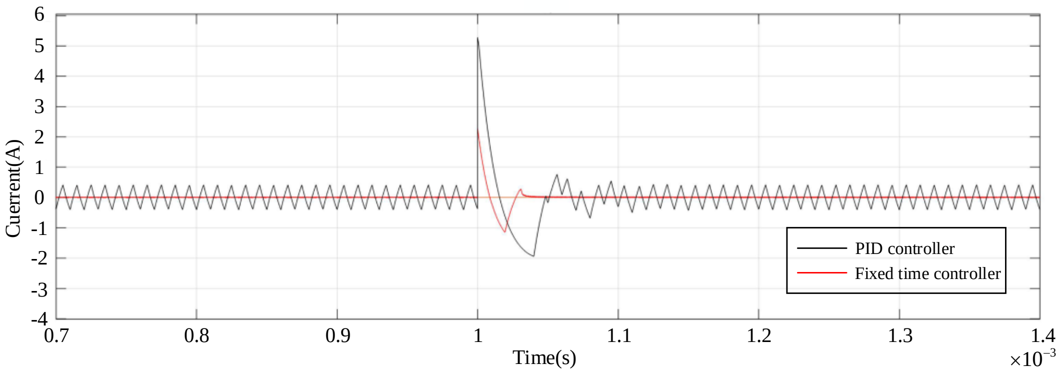

Fig. 4 – Comparison of output current ripple between two controllers under load changes.

2) *Simulation under changes in input voltage*. Similarly, to assess the tracking capabilities of the proposed controller and PID controller concerning output voltage and output current ripple under varying input voltage, step changes are introduced at 2 ms and 4 ms. Specifically, at 2 ms, the input voltage changes from 40 V to 48 V, and at 4ms, it changes from 48 V to 40 V. Figure 5 illustrates that in the presence of input voltage changes, the disturbance observer accurately estimates the input voltage, enabling the proposed controller to swiftly track the reference output voltage. Compared to the PID control, the proposed controller demonstrates a faster response speed (increased by 15.4%) and reduced overshoot (decreased by 13.3%). Furthermore, as depicted in Fig. 6, the designed controller exhibits minimal impact on the bidirectional DC-DC circuit and generates smaller ripple compared to the traditional PID control.

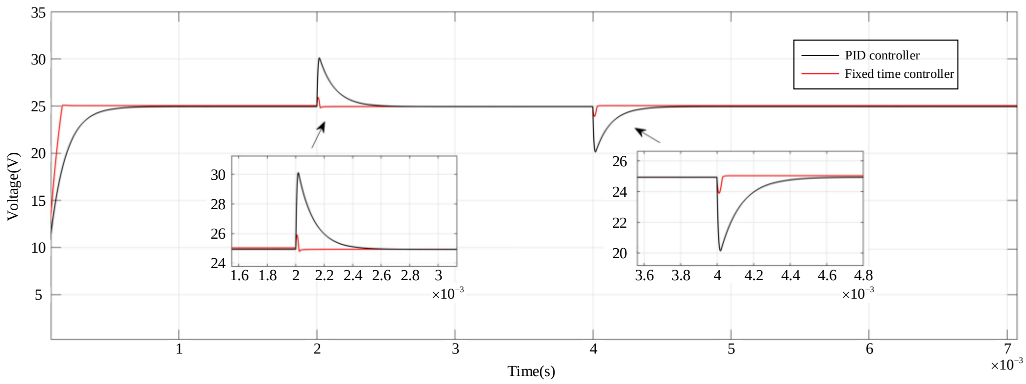

Fig. 5 – Comparison of output voltage tracking effects between two controllers under changes in input voltage.

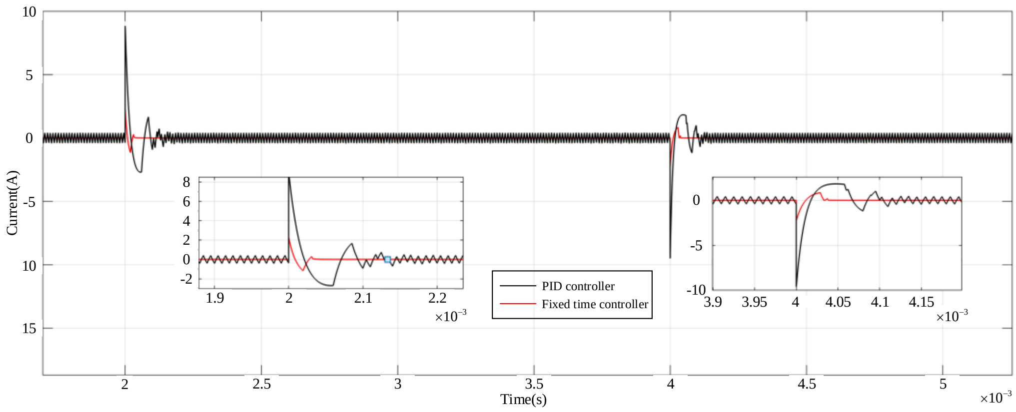

Fig. 6 – Comparison of output current ripple between two controllers under changes in input voltage.

3) *Simulation comparison of disturbance observer*. To verify the effectiveness of the disturbance observer, the resistance value changes from 10 Ω to 13 Ω at 2 ms. Figure 7 compares the performance of the disturbance observer. When the load changes, the observer can accurately and quickly track the estimated

value, and the speed is related to the gain. Compared to the observation gain value of 10, when the observation gain value is 100, the estimated value can approach the actual value faster. Figure 8 compares the performance of a fixed time controller with a fixed time controller with a disturbance observer. Due to the observer's ability to compensate for changes in resistance, a fixed time controller with a disturbance observer can track the reference voltage faster than a fixed time controller without disturbance observers. The adjustment time is reduced by 22.8%.

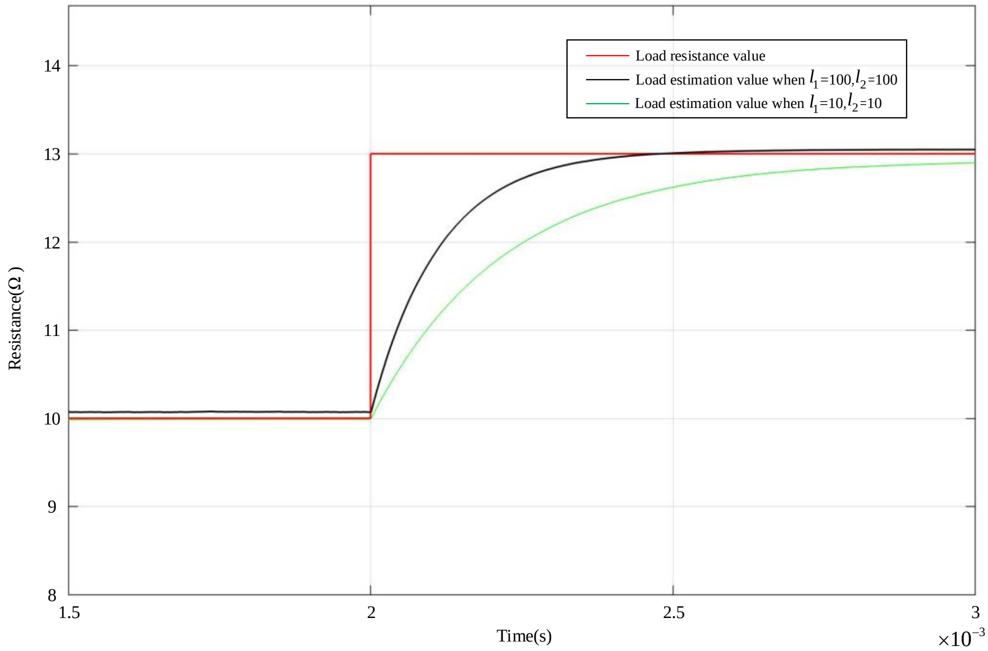

Fig. 7 – The effect of different observer gains on the performance of disturbance observer.

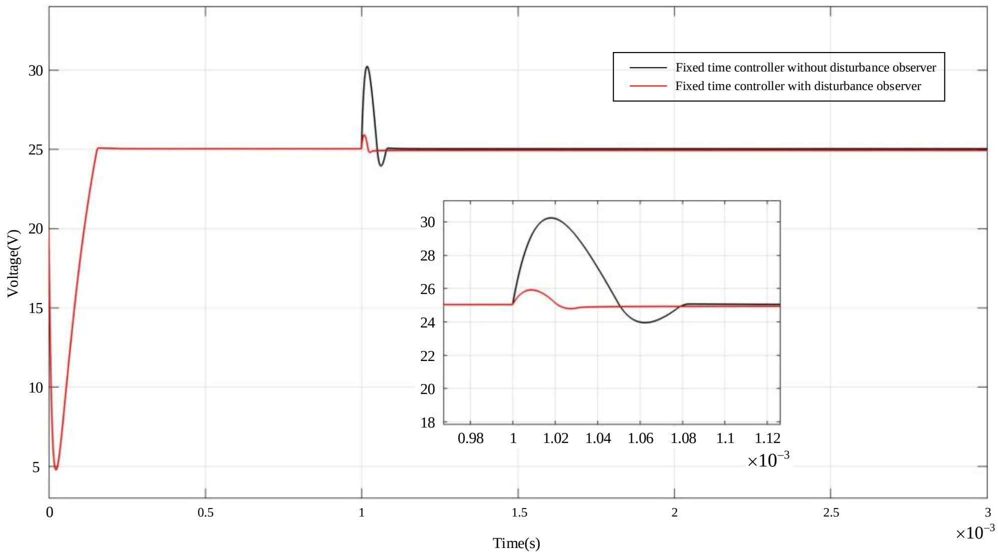

Fig. 8 – Comparison of fixed time controllers with and without disturbance observers.

4.2. Experiment results

To validate the effectiveness of the designed controller, a hardware circuit is constructed, as illustrated in Fig. 9. This circuit comprises a bidirectional DC-DC circuit, a voltage and current sampling circuit, and a control circuit(dSPACE-DS1202). With an input voltage of 40 V, a resistance of 25 **Ω**, and a target voltage of 25 V, the dSPACE-DS1202 generates PWM signals that are passed through the driving circuit and then applied to the bidirectional DC-DC circuit.

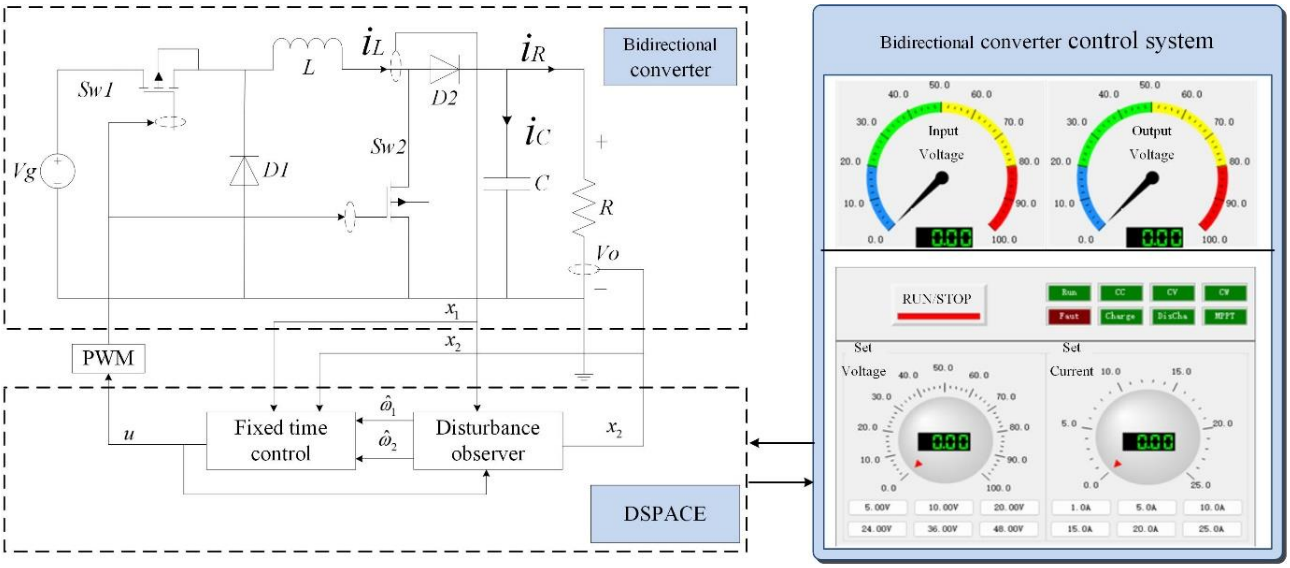

Fig. 9 – Hardware testing platform.

In practical implementation, the effectiveness of the algorithm is verified by evaluating its ability to quickly track the reference voltage. As shown in Fig. 10a and Table 3, the proposed control strategy exhibits superior performance in terms of adjustment time and overshoot compared to PID controllers. The adjustment time is reduced by 17.8% and overshoot is reduced by 20.8%, providing convincing evidence for the advantageous fast adjustment ability of the proposed controller. To demonstrate the effectiveness of the observer, the resistance changed from 25 Ω to 28 Ω ohms at 0.6 s in Fig. 10b. It can be seen that the proposed control algorithm reduces the adjustment time by 18.9% and the overshoot by 22.7% compared to the PID controller.

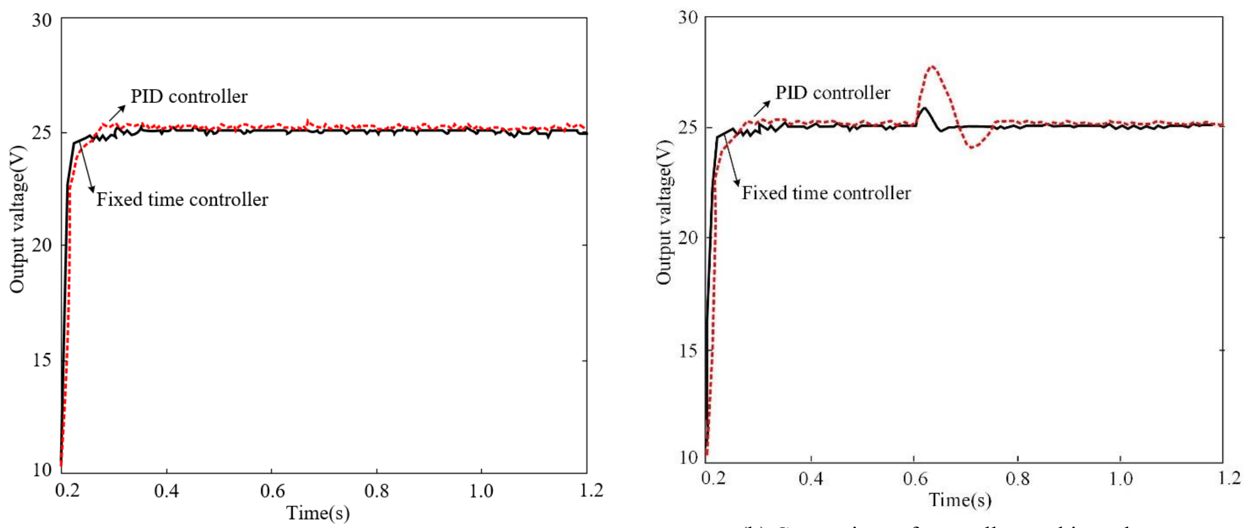

(a) Comparison of controller tracking with constant load resistance

(b) Comparison of controller tracking when load resistance changes

Fig. 10 – Two controllers in practical circuits for tracking reference voltage effects.

Table 3

Comparison of the effects of two controllers

Method	Overshoot (V)	Settling Time (ms)
PID controller	0.48	330.3
Fixed time controller	0.38	271.5

5. CONCLUSION

In this paper, a fixed time composite controller is designed based on a disturbance observer and implemented in a bidirectional DC-DC converter. The objective is to enhance the system's dynamic performance in the presence of external interference and uncertainty. The proposed disturbance observer effectively compensates for input voltage and load disturbances, while the fixed time controller achieves rapid tracking and adjustment of the output voltage without requiring measurements of input voltage and load current. The proposed method has been effectively verified through simulation and experiments to improve the convergence speed of the system and reduce current ripple under changes in load and input voltage.

ACKNOWLEDGMENTS

This work was supported in part by the National Natural Science Foundation of China under Grant (62301212,62371182), the Program for Science and Technology Innovation Talents in the University of Henan Province under Grant(23HASTIT021), Major Science and Technology Projects of Longmen Laboratory under Grant(231100220300), Aeronautical Science Foundation of China under Grant(20220001042002), the Science and Technology Development Plan of Joint Research Program of Henan under Grant(225200810007, 222103810036), the Scientific and Technological Project of Henan Province under Grant(222102240009).

REFERENCES

[1] Rose JL, Sankaragomathi B. Comparison of Buck-Boost and Ćuk converters based on time domain response. Journal of Circuits, Systems and Computers 2018;27(14):41–60.
[2] Shanmugam SK, Muthusamy K, Sennippan V, Balasubramaniam S, Ramasamy S. Modelling of solar photovoltaic array fed brushless DC motor drive using enhanced DC-DC converter. Proceedings of the Romanian Academy, Series A 2019;20(2):169–178.
[3] Siddhartha V, Hote YV. Low-power non-ideal pulse-width modulated DC-DC buck-boost converter: design, analysis and experimentation. IEICE Transactions on Communications 2009;92(3):998–1003.
[4] Nagaiah M, Sekhar KC. Analysis of fuzzy logic controller based bi-directional DC-DC converter for battery energy management in hybrid solar/wind micro grid system. International Journal of Electrical and Computer Engineering 2020;10(3):2271–2284.
[5] Wang B, Qin F, Zhao X. Equalization of series connected lithium-ion batteries based on back propagation neural network and fuzzy logic control. International Journal of Energy Research 2020;44(6):2148–2160.
[6] Şahin ME, Okumuş Hİ. Comparison of different controllers and stability analysis for photovoltaic powered Buck-Boost DC-DC converter. Electric Power Components & Systems 2018;46(4):149–161.
[7] Tekin H, Bulut K, Ertekin D. A novel switched-capacitor and fuzzy logic-based quadratic boost converter with mitigated voltage stress, applicable for DC micro-grid. Electrical Engineering 2022;104(6):4391–4413.
[8] Sakthivel K, Krishnasamy R, Balasubramanian K, Krishnakumar V, Ganesan M. Averaged state space modeling and the applicability of the series compensated Buck-Boost converter for harvesting solar photo voltaic energy. Sustainable Energy Technologies and Assessments 2022;53(C):102611.
[9] Su M, Feng W, Jiang T, Guo B, Wang H, Zheng C. Disturbance observer-based sliding mode control for dynamic performance enhancement and current-sensorless of buck/boost converter. IET Power Electronics 2021;14(8):1421–1432.
[10] Cheng Z, Li Z, Li S, Gao J, Dong W. A novel cascaded control to improve stability and inertia of parallel buck-boost converters in DC microgrid. International Journal of Electrical Power & Energy Systems 2020;119(4):2966–2977.
[11] Zheng S, Qi M, Shu Y, Wang Y, Lang J. Non-singular terminal sliding mode control strategy for DC/DC Boost converter system using a finite-time convergent observer. IET Power Electronics 2022;15(16):1868–1876.
[12] Pandey SK, Patil SL, Phadke SB. Regulation of nonminimum phase DC-DC converters using integral sliding mode control combined with a disturbance observer. IEEE Transactions on Circuits and Systems II: Express Briefs 2017;65(11): 1649–1653.
[13] Łakomy K, Madonski R, Dai B, Yang J, Kicki P, Ansari M, Li S. Active disturbance rejection control design with suppression of sensor noise effects in application to DC-DC Buck power converter. IEEE Transactions on Industrial Electronics 2021;69(1): 816–824.
[14] Wang N, Tao F, Fu Z, Song S. Adaptive fuzzy control for a class of stochastic strict feedback high-order nonlinear systems with full-state constraints. IEEE Transactions on Systems, Man, and Cybernetics: Systems 2020;52(1):205–213.
[15] Wang N, Fu Z, Song S, Wang T. Barrier-Lyapunov-based adaptive fuzzy finite-time tracking of pure-feedback nonlinear systems with constraints. IEEE Transactions on Fuzzy Systems 2022;30(4):1139–1148.

[16] Tian X, Tao F, Fu Z, Wang N, Song S. Fixed time control based on finite time observer for Buck converter system with load disturbance. Control Engineering and Applied Informatics 2023;25(1):3–11.
[17] Wang J, Li S, Yang J, Wu B, Qi L. Extended state observer-based sliding mode control for PWM-based DC-DC buck power converter systems with mismatched disturbances. IET Control Theory & Applications 2015;9(4):579–586.
[18] Wang J, Rong J, Yu L. Reduced-order extended state observer based event-triggered sliding mode control for DC-DC buck converter system with parameter perturbation. Asian Journal of Control 2021;23(3):1591–1601.
[19] Zhuo S, Gaillard A, Xu L, Paire D, Gao F. Extended state observer-based control of DC–DC converters for fuel cell application. IEEE Transactions on Power Electronics 2020;35(9):9923–9932.
[20] Kim SK. Proportional-type output voltage-tracking controller for interleaved DC/DC Boost converter with performance recovery property. Mathematical Problems in Engineering 2018;1(12):2094–2100.
[21] Xu Q, Vafamand N, Chen L, Dragičević T, Xie L, Blaabjerg F. Review on advanced control technologies for bidirectional DC/DC converters in DC microgrids. IEEE Journal of Emerging and Selected Topics in Power Electronics 2021;9(2):1205–1221.
[22] Van Gorp J, Defoort M, Djemai M, Veluvolu KC. Fault detection based on higher-order sliding mode observer for a class of switched linear systems. IET Control Theory & Applications 2015;9(15):2249–2256.
[23] Pandey SK, Veeranna K, Patil SL, Phadke SB. Uncertainty estimator based sliding mode control schemes for multimode noninverting Buck-Boost DC-DC converter. IFAC-PapersOnLine 2020;53(1):555–560.
[24] Ju H, Tao F, Wang N, Ma H. Observer-based fixed-time fuzzy tracking control for stochastic nonstrict nonlinear systems with hysteresis nonlinearity. Transactions of the Institute of Measurement and Control 2023;45(11):2122–2134.

Received September 5, 2023